

# Analysis of RLV's Coupling Characteristic and Control Strategy Design

Shi Linan<sup>\*</sup>, Wang Zhi and Li Zhaoying

School of Astronautics, Beihang University, Beijing, China, 100191, P.R. China

**Abstract:** Reusable launch vehicle (RLV) in the reentry process exhibit fast time-variation, strongly nonlinear and coupling characteristics, they all increase the complexity of attitude control system. After a vehicle's mathematical model is built for the analysis of RLV movement and attitude control system design, then some operating points are selected from the trajectory and linearized. Several common coupling mechanisms are described, including the inertial coupling, the motion coupling, the Dutch coupling and the control coupling. Calculation results of rapid roll stability boundary are given, and a criterion of the Dutch-roll motion stabilization is proposed. Based on the analysis of the coupling characteristics, a RLV longitudinal and lateral/directional motion control strategy is designed: elevators are used to trim and control on the longitudinal channel; body flaps and RCS are used to hybrid control on the lateral/direction channel at low dynamic pressure and at high dynamic pressure body flaps can work alone. Finally, the 6 DOF simulation results prove the validity of the control strategy.

**Keywords:** RLV, lateral coupling, Dutch roll coupling, attitude control strategy.

## 1. INTRODUCTION

Reusable launch vehicle flies in supersonic speed during reentry, it has complex flight dynamics, strong nonlinearity and coupling characteristics [1-3]. Especially for lateral/direction channel, due to its fast flight speed, even slow development of coupled instability is also likely to evolve into a rapidly growing coupled instability which leads to a strong uncontrollable movement of the vehicle. For instance X-2 aircraft in the reentry process has control coupling, inertial coupling and spin; X-15 suffered the decrease of stability of the Dutch roll and unstable control mode; Space Transportation System (STS) experienced control coupling and Dutch roll coupling in supersonic and superb reentry process [4].

In the previous study actual coupling effects are often been simplified. They are considered as a number of simple systems, or some coupling phenomena are ignored directly. But with the increase of the complexity of the system and the requirement of the performance, this procedure is often proved inappropriate [5]. Therefore, the study of the mechanism and generating conditions of coupling phenomenon and the design of attitude control strategy aiming at RLV's coupling characteristics is necessary. Instead of common decoupling control strategy, this paper is based on the analysis of coupling characteristics of the aircraft and designs a coordinated control strategy for lateral/directional channel. First, for a certain shape of RLV, the rigid attitude dynamics equations are established then the model is trimmed and linearized. The causes and mechanism of several common couplings of these aircraft are analyzed, and the corresponding countermeasures of the coupling phenomena are given.

Next, attitude control strategy which considers coupling characteristics and aiming at simplification of the control law structure and decreasing of the RCS fuel consumption is designed. Finally, six degrees of freedom simulation results have verified the feasibility of the control strategy.

## 2. THE MATHEMATICAL MODEL OF RLV

The rigid attitude dynamics equations of unpowered reentry vehicle are shown in equation 1. The state vector is  $x = [\alpha \ \beta \ \mu \ p \ q \ r]^T$  which denotes respectively the angle of attack, sideslip angle, bank angle, roll rate, pitch rate and yaw rate. The control input vector is  $u = [\delta_e \ \delta_a \ L_{RCS} \ M_{RCS} \ N_{RCS}]^T$  which denote respectively elevator angle, aileron angle and the output torques of the RCS system projected on three axis of body coordinate. The differential equations of angle of attack and sideslip angle and bank angle established under the relative coordinate while the differential equations of attitude angular rate established under the inertial system. Due to the gravitational acceleration, bank angle and flight path angle change more slowly than the attitude angle and attitude angular rate, so they are treated as constants [6]. The damping derivative is ignored in the model, namely the derivatives like  $Y_\delta$  and  $L_\delta$  are set to zero. It is an advisable assumption to the lifting body aircraft under hypersonic flight state.

$$\begin{aligned}\dot{\alpha} &= -p \cos \alpha \tan \beta + q - r \sin \alpha \tan \beta + \frac{g \cos \mu \cos \gamma}{V \cos \beta} - \frac{L}{mV \cos \beta} \\ \dot{\beta} &= \frac{Y}{mV} + \frac{g \sin \phi \cos \alpha}{V} - r \cos \alpha + p \sin \alpha \\ \dot{\mu} &= p \cos \alpha \frac{1}{\cos \beta} + r \sin \alpha \frac{1}{\cos \beta} + \frac{L \tan \beta}{mV} - \frac{g \tan \beta}{V} \cos \mu \cos \gamma \\ &\quad + \frac{\tan \gamma}{mV} (Y \cos \mu + L \sin \mu)\end{aligned}$$

<sup>\*</sup>Address correspondence to this author at the School of Astronautics, Beihang University, Beijing, China, 100191, P.R. China; Tel: 8610-82339527; E-mail: shi\_linan@163.com

$$\begin{aligned}\dot{p} &= \frac{I_{xz}(I_x - I_y + I_z)pq + (I_y I_z - I_z I_x - I_{xz} I_{xz})qr + I_z L_A + I_{xz} N_A}{I_x I_z - I_{xz} I_{xz}} \\ \dot{q} &= \frac{-(I_x - I_z)pr - I_{xz}(p^2 - r^2) + M_A}{I_y} \\ \dot{r} &= \frac{(I_x I_x - I_x I_y + I_{xz} I_{xz})pq + I_{xz}(-I_x + I_y - I_z)qr + I_x N_A + I_{xz} L_A}{I_x I_z - I_{xz} I_{xz}}\end{aligned}\quad (1)$$

Usually the roll angle command given from guidance system is under the stable coordinate system. The actuator is installed in the vehicle body coordinate system and by changing the attitude angular rate so that the aircraft attitude changes. Therefore we use the attitude roll angle which rotated around the x-axis of body coordinate when analyze the attitude of the aircraft, therefore we need to know the tracking performance of bank angle  $\mu$  during the six-degree of freedom simulation. Consequently the dynamic of attitude roll angle equation is added as follows:

$$\dot{\phi} = p + (q \sin \phi + r \cos \phi) \tan \alpha \quad (2)$$

Then trim the attitude equations on the equilibrium points in the reentry trajectory and then linearization the model in order to obtain the longitudinal and lateral linear model as follows:

$$\begin{bmatrix} \dot{\alpha} \\ \dot{q} \end{bmatrix} = \begin{bmatrix} -\bar{Z}_\alpha & 1 \\ \bar{M}_\alpha & \bar{M}_q \end{bmatrix} \begin{bmatrix} \alpha \\ q \end{bmatrix} + \begin{bmatrix} -\bar{Z}_{\delta_e} & 0 \\ \bar{M}_{\delta_e} & 1/I_y \end{bmatrix} \begin{bmatrix} \delta_e \\ M_{RCS} \end{bmatrix} \quad (3)$$

$$\begin{bmatrix} \dot{\beta} \\ \dot{\phi} \\ \dot{p} \\ \dot{r} \end{bmatrix} = \begin{bmatrix} \bar{Y}_\beta & g \cos \alpha / V & \bar{Y}_p + \sin \alpha & \bar{Y}_r - \cos \alpha \\ 0 & 0 & 1 & \tan \alpha \\ \bar{L}_\beta & 0 & \bar{L}_p & \bar{L}_r \\ \bar{N}_\beta & 0 & \bar{N}_p & \bar{N}_r \end{bmatrix} \begin{bmatrix} \beta \\ \phi \\ p \\ r \end{bmatrix} + \begin{bmatrix} \bar{Y}_{\delta_e} & 0 & 0 \\ 0 & 0 & 0 \\ \bar{L}_{\delta_e} & I_z/I_\Delta & I_{xz}/I_\Delta \\ \bar{N}_{\delta_e} & I_{xz}/I_\Delta & I_x/I_\Delta \end{bmatrix} \begin{bmatrix} \delta_e \\ L_{RCS} \\ N_{RCS} \end{bmatrix} \quad (4)$$

where  $\bar{Z}_\alpha = Z_\alpha / mV$ ,  $\bar{Z}_{\delta_e} = Z_{\delta_e} / mV$ ,  $\bar{M}_i = M_i / I_y$

$$(i = \alpha, q, \delta_e), I_\Delta = I_x I_z - I_{xz} I_{xz}, \bar{L}_j = \frac{N_j (I_{xz} / I_z) + L_j}{I_x - (I_{xz}^2 / I_z)},$$

$$\bar{N}_j = \frac{N_j + L_j (I_{xz} / I_x)}{I_z - I_{xz}^2 / I_x}, \bar{Y}_j = \frac{Y_j}{mV} \quad (j = \beta, p, r, \delta_e).$$

### 3. THE SUMMARIZE OF COUPLING

#### 3.1. The Inertial Coupling

Inertial coupling is the situation that the adverse moment of inertia will be produced when the aircraft is not roll about its principal axis of inertia. Extra pitch moment of inertia  $(I_x - I_z)pr$  and yaw moment of inertia  $(I_y - I_x)pq$  will be produced and offset part of the original static stability moment in pitch and yaw channels when the roll rate  $p$  is large

enough. Similarly, when there is a pitch rate  $q$ , additional adverse rolling moment  $(I_z - I_y)qr$  and yawing moment  $(I_y - I_x)pq$  will be produced in the roll and yaw channels.

Now we assume that the aircraft roll around a horizontal straight line at a given constant speed, then linearize the dynamics equations rotating around center of gravity and the dynamics equations of motion of center of gravity under the body coordinates, after ignoring the products of inertia and high order quantities, the matrix forms of linear equation is obtained as follows:

$$\begin{bmatrix} \Delta \dot{\alpha} \\ \Delta \dot{\beta} \\ \Delta \dot{q} \\ \Delta \dot{r} \end{bmatrix} = \begin{bmatrix} 0 & -p_* & 1 & 0 \\ p_* & 0 & 0 & -1 \\ \bar{M}_\alpha & 0 & \bar{M}_q & (I_z - I_x)p_*/I_y \\ 0 & \bar{N}_\beta & (I_x - I_y)p_*/I_z & \bar{N}_r \end{bmatrix} \begin{bmatrix} \Delta \alpha \\ \Delta \beta \\ \Delta q \\ \Delta r \end{bmatrix} + \begin{bmatrix} 0 & 0 \\ 0 & 0 \\ \bar{M}_{\delta_e} & 0 \\ 0 & \bar{N}_{\delta_e} \end{bmatrix} \begin{bmatrix} \Delta \delta_e \\ \Delta \delta_a \end{bmatrix} \quad (5)$$

The characteristic equation is:

$$s^4 + as^3 + bs^2 + cs + d = 0 \quad (6)$$

Ignoring the damping terms  $M_q, N_r$ , the characteristic equation can be simplified to  $s^4 + bs^2 + d = 0$ , where:

$$\begin{aligned}b &= \bar{N}_\beta - \bar{M}_\alpha + \left(1 - \left(\frac{I_z - I_x}{I_y}\right)\left(\frac{I_x - I_y}{I_z}\right)\right)p_*^2 \\ d &= \left(\left(\frac{I_z - I_x}{I_y}\right)p_*^2 + \bar{M}_\alpha\right)\left(-\left(\frac{I_x - I_y}{I_z}\right)p_*^2 - \bar{N}_\beta\right)\end{aligned}\quad (7)$$

It is obviously that the rapid roll stability conditions are  $b > 0$  and  $d > 0$ .  $1 - (I_z - I_x)(I_x - I_y)/I_y I_z$  generally greater than zero meanwhile this kind of vehicle has the yaw static stability and the longitudinal static stability under high Mach number case (namely  $\bar{N}_\beta > 0$  and  $\bar{M}_\alpha < 0$ ) make the guarantee of  $b > 0$ . Consequently, let  $d > 0$  we can obtain the necessary condition of the steady roll-in as follows:

$$\left(\left(\frac{I_z - I_x}{I_y}\right)p_*^2 + \bar{M}_\alpha\right)\left(-\left(\frac{I_x - I_y}{I_z}\right)p_*^2 - \bar{N}_\beta\right) > 0 \quad (8)$$

let  $\omega_A^* = -\bar{M}_\alpha I_y / (I_z - I_x)$ ,  $\omega_B^* = \bar{N}_\beta I_z / (I_y - I_x)$ , then

$$p_*^2 > \omega_A^* \text{ and } p_*^2 > \omega_B^* \text{ or } p_*^2 < \omega_A^* \text{ and } p_*^2 < \omega_B^* \quad (9)$$

Fig. (1) is the vehicle's rapid roll stability boundary according to formula (9). Where the purple and green regions represent the stability region while the blue part is the yaw and pitch divergence region respectively.

Now we calculate  $\omega_A^*$  and  $\omega_B^*$ , as shown in Fig. (2), on the equilibrium points on the reentry trajectory which have longitudinal static stability.

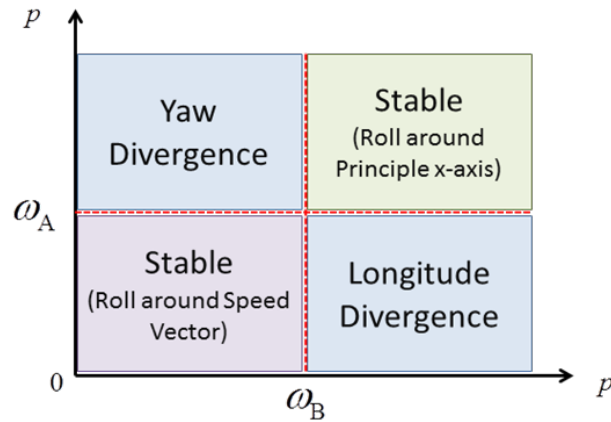


Fig. (1). The roll stable boundary.

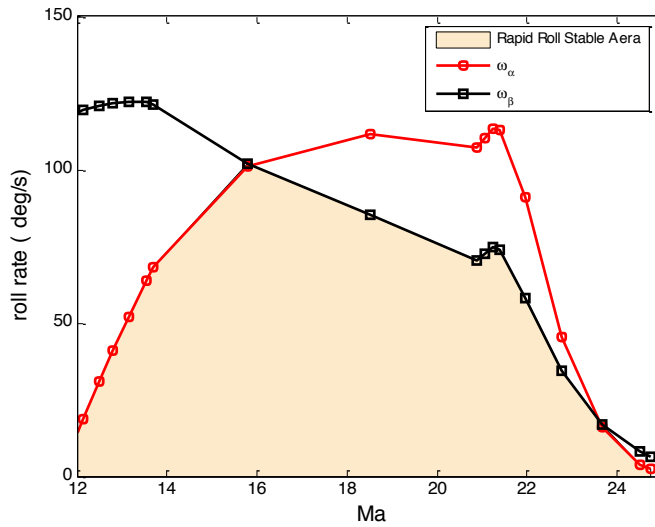


Fig. (2). The roll stable boundary along a trajectory.

According to the previous analysis, the vehicle's roll rate should be less than  $\min(\omega_A^*, \omega_B^*)$ . Therefore in Fig. (2), the shadow area represents the rapid roll stability region. As can be seen from the Fig. (2), the roll angle velocity constraint required by longitudinal channel is very small and plays a dominant role at the initial descent phase, consequently it should try to avoid large rolling maneuvers at this period. At high Mach number gliding period, the roll angle velocity constraint required by yaw channel is more important. In other words, yaw channel is more likely to divergence due to large roll rate at this period. Therefore, in the design proceeding of the vehicle's control law, the inertial coupling can be improved through the roll rate limitation. For instance, the space shuttle's limited its roll rate and had the similar characteristics with Fig. (2).

### 3.2. The Motion Coupling

Because of the existence of movement coupling when hypersonic vehicle roll under high angle of attack, angle of

attack and sideslip angle will transform into each other, and this conversion is the one of the causes of unstable rapid roll. The degree of movement generally depends on the roll rate [7]:

$$\begin{aligned} \dot{\alpha} &= q - \tan \beta (p \cos \alpha + r \sin \alpha) \\ \dot{\beta} &= p \sin \alpha - r \cos \alpha \end{aligned} \tag{10}$$

If you want to remain  $\alpha$  the same, it should maintain sideslip angle at zero according to equation (10), If you want to remain  $\beta$  the same, the vehicle should roll around the x-axis of the stable coordinate system instead of body coordinate and maintain the projection of velocity on the z-axis of the stable coordinate system at zero at the same time, that is  $r_s = r \cos \alpha - p \sin \alpha = 0$ . Therefore the roll rate and yaw rate at body coordinate system must satisfy the following relationship:

$$p = r \cot \alpha \tag{11}$$

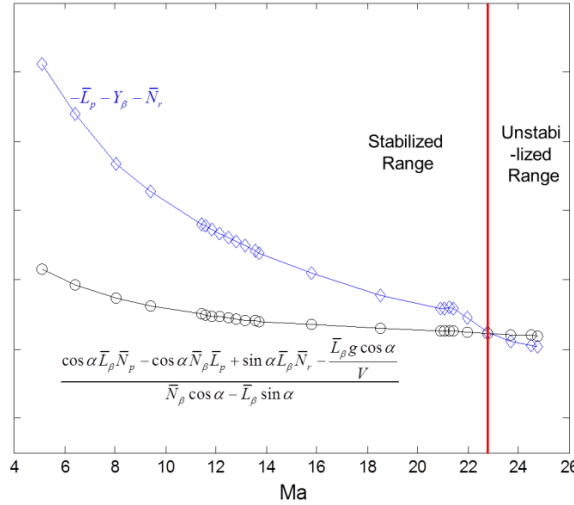


Fig. (3). The dutch roll damping decomposition.

This means the movement coupling will not exist when the roll rate is  $\cot \alpha$  times of the yaw rate.

### 3.3. The Dutch Roll Coupling

There are usually three kinds of modes in the lateral movement of aircraft: Dutch roll mode, roll convergence mode and spiral mode. The Dutch roll mode is coupling of the rolling movement and yawing movement. Roll-spiral coupling, occurs at the initial phase of reentry, is a long-period motion generates as a result of the coupling of the rolling movement and the spiral movement [8]. This section focuses on the analysis of such common Dutch coupling phenomena.

The Dutch roll mode is coupling of the rolling movement and yawing movement. The dynamic yaw stability derivative  $C_{n,dyn}^\beta$  is used to characterize the yaw dynamic stability (the Dutch roll stability). The vehicle has yaw dynamic stability when  $C_{n,dyn}^\beta > 0$ .

$$C_{n,dyn}^\beta = \left( \frac{C_n^\beta + \frac{I_{xz}}{I_x} C_l^\beta}{1 - \frac{I_{xz}^2}{I_x I_z}} \right) \cos \alpha - \frac{I_z}{I_x} \left( \frac{C_l^\beta + \frac{I_{xz}}{I_z} C_n^\beta}{1 - \frac{I_{xz}^2}{I_x I_z}} \right) \sin \alpha \quad (12)$$

As can be seen from the equation (12),  $C_{n,dyn}^\beta$  includes the influences of the reverse effect, angle of attack and inertia ratio on the Dutch roll. The Dutch roll frequency can be predicted as follows:

$$\omega_d^2 \approx Q S b C_{n,dyn}^\beta / I_{zz} \quad (13)$$

The lateral characteristic equation is obtained from the linear model (4) with ignoring the influences of damping torque and attitude angular rate on side force [9]:

$$|sI - A| = s^2 (s^2 - \bar{Y}_\beta s + \cos \alpha \bar{N}_\beta - \sin \alpha \bar{L}_\beta) \quad (14)$$

The eigenvalues of the roll mode and spiral mode degenerate to zero after such simplify [10]. The constant term in the equation above is the square of the Dutch roll frequency. This illustrates that  $C_{n,dyn}^\beta > 0$  is only a sufficient condition for stability of the Dutch roll. In this paper, a predication method of Dutch roll frequency is presented in equation (15), and the prediction result along the reentry trajectory is shown in Fig. (3).

$$2\xi_d \omega_d = -\bar{L}_p - Y_\beta - \bar{N}_r - \frac{\cos \alpha \bar{L}_\beta \bar{N}_p - \cos \alpha \bar{N}_\beta \bar{L}_p + \sin \alpha \bar{L}_\beta \bar{N}_r - \frac{\bar{L}_\beta g \cos \alpha}{V}}{\bar{N}_\beta \cos \alpha - \bar{L}_\beta \sin \alpha} \quad (15)$$

As shown in Fig. (3), the prediction result using equation (15) is consistent with the results of mode analysis. The equation (15) can predict the stability of the Dutch roll mode. The equation (15) can be simplified as

$$2\xi_d \omega_d = -Y_\beta + \frac{\bar{L}_\beta g \cos \alpha}{V (\bar{N}_\beta \cos \alpha - \bar{L}_\beta \sin \alpha)} \quad \text{when the damping}$$

torque is small, the larger  $Y_\beta$  on magnitude and more strongly reverse effect will help stabilize the Dutch roll mode.

### 3.4. The Control Coupling

When both body flaps deflect differentially there will produce extra adverse yaw moment besides desired roll moment and the so-called aileron reverse effect phenomenon will appeared that an aircraft rolled to the right while

manipulate body flaps to make the vehicle roll around to the left. The Lateral Control Departure Parameter (LCDP) is used to predict the aileron performance [11, 12]:

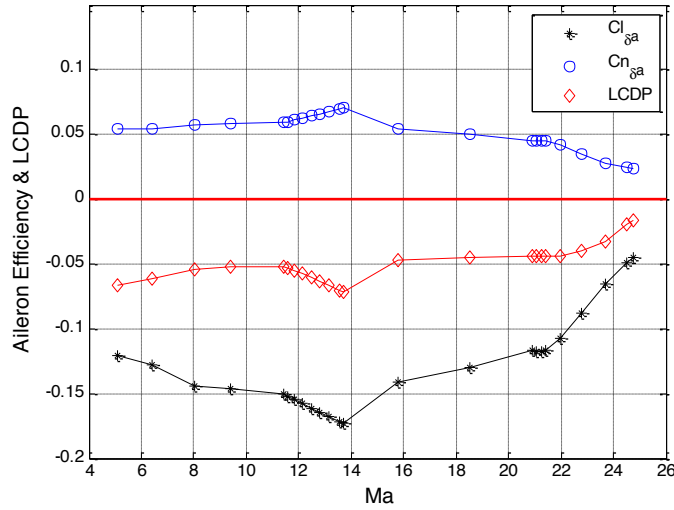


Fig. (4). The aileron efficiency & LCDP along a trajectory.

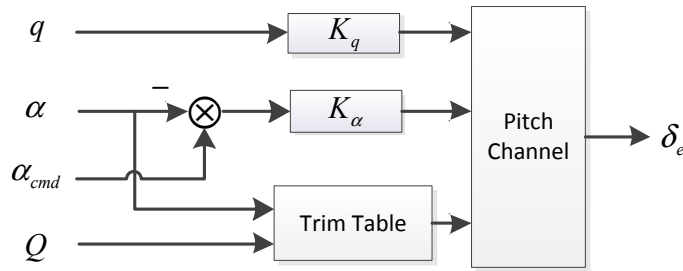


Fig. (5). The longitudinal control strategy.

$$LCDP = C_n^\beta - \frac{C_l^\beta C_n^{\delta_a}}{C_l^{\delta_a}} \tag{16}$$

The transfer function of aileron to roll rate (17) can be easily obtained for a linear system. In general cases  $QSb \cos \alpha / I_{zz} > 0$ , so the roll channel is stable when  $LCDP > 0$ . The system is a non-minimum phase system when  $LCDP < 0$  and the roll command cannot be accurately tracked.

$$\frac{p}{\delta_a} = \frac{(QSb C_{l_{\delta_a}} / I_{xx}) \left( s^2 + \frac{QSb}{I_{zz}} \left( C_{n\beta} \cos \alpha - \frac{C_{l\beta} C_{n\delta_a}}{C_{l_{\delta_a}}} \cos \alpha \right) \right)}{\Delta} \tag{17}$$

$$= \frac{(QSb C_{l_{\delta_a}} / I_{xx}) \left( s^2 + \frac{QSb \cos \alpha}{I_{zz}} LCDP \right)}{\Delta}$$

There are two main reason of negative LCDP: insufficient stability/unstable yaw movement or  $C_n^{\delta_a} > 0$ . Because the space shuttle does not have the yaw stability, the sideslip angle caused by the adverse yaw moment keeps diverging and the roll moment motivated by the sideslip angle will impede the desire aileron roll control with the existence of reverse effect. The object vehicle of this paper has yaw stability and  $C_n^{\delta_a} > 0$ , as shown in Fig. (4), so positive aileron deflection will produce desired negative roll moment mean-

while additional positive adverse yaw moment will motivate negative sideslip angle. Furthermore, a positive roll moment will be generated to obstacle the effect of aileron roll control by this negative sideslip angle under strongly reverse effect or even cause a positive roll movement.

#### 4. THE CONTROL STRATEGY DESIGN

The actuators of the object vehicle of this paper are body flaps and RCS system. The RCS system is non-redundant system, and in the aerodynamic actuators-only control period two control surfaces control three channels make the system a typical under actuated system. With the purpose of simpler control system structure and less RCS propellant consumption, in this section we propose body flaps-RCS hybrid control strategy in low dynamic pressure and body flaps used alone lateral/directional control strategy in high dynamic pressure.

##### 4.1. The Longitudinal Control Strategy

The equations of aircraft longitudinal short period linear model are shown in (3), the control input of the model are elevator deflection and pitch moment of RCS system. The longitudinal movement is stable but has small damping when

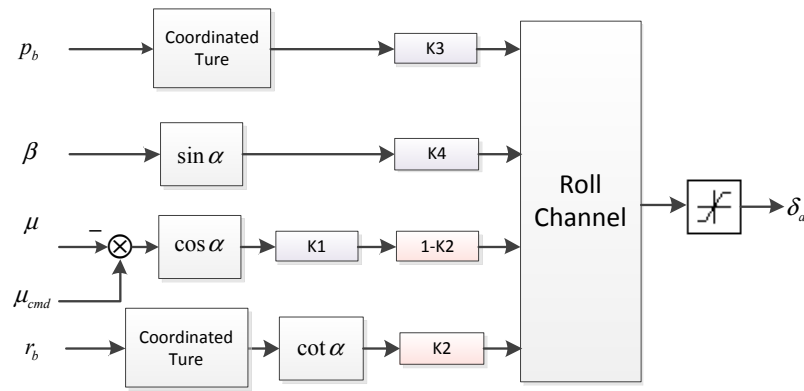


Fig. (6). The roll channel control strategy (low dynamic pressure).

the Mach number is larger than 12. The longitudinal control strategy is designed as shown in Fig. (5).

The trim elevator deflection is obtained through online interpolation according to the current angle of attack and dynamic pressure. The tracking of angle of attack is achieved through the feedback of the error of angle of attack and its command  $e_{\Delta\alpha}$ , while longitudinal stabilizing is realized through the feedback of pitch rate  $q$ . Adjusting control parameters  $K_q$  and  $K_\alpha$  to obtain adequate natural frequency and damping ratio of the short-period motion Pitch rate feedback can provide sufficient damping in longitudinal hence we only use elevator actualize trim and attitude control to save RCS propellant. But RCS control channel should be retained in case of fault status or disturbance.

#### 4.2. The Lateral/Directional Control Strategy

##### 4.2.1. Low Dynamic Pressure: Aileron-RCS Hybrid Control Strategy

The Dutch roll mode of the object vehicle is unstable at high Mach numbers which greater than 22, and its damping is very small in the whole entry process. As a consequence the lateral attitude control is to stabilize the Dutch roll mode at high Mach numbers and to increase damping in the entire entry process.

In order to solve the problem of motion coupling and maintain zero sideslip angle and yaw rate when hypersonic vehicle is in the process of rolling maneuvers with large angle of attack, the vehicle should roll around the x axis of speed coordinates and maintain zero yaw rate under this coordinates. On this condition the roll and yaw rate in the body coordinates must satisfy  $p_b = r_b \cot\alpha$ . Consequently for the purpose of reducing motion coupling the yaw rate is feedback to roll damping channel.

The guidance command is obtained under the speed coordinates including angle of attack, sideslip angle and bank

angle. The actuators are installed under the body coordinate system so they can only response the command under the same coordinate. Therefore guidance commands should be projected to the body coordinates before sent to the control system. Namely the sideslip angle and bank angle commands should be projected respectively on the roll channel as  $-\beta\sin\alpha$  and  $\mu\cos\alpha$  while on the yaw channel as  $\beta\cos\alpha$  and  $\mu\sin\alpha$

The Dutch roll mode is unstable in the early reentry phase and the damping is very small. Because the roll movement plays a dominant role in the Dutch roll mode, the roll rate feedback to aileron will provide necessary damping thereby the Dutch roll mode is stabled.

The vehicle's LCDP is less than zero means there has aileron reversal phenomenon during the entire reentry. LCDP varies notable with angle of attack, even in flight nearby 80km and 10°angle of attack, LCDP will change from negative to positive namely there's not aileron reversal ever. For the purpose of avoiding the controller failure risks due to the uncertainty of LCDP, this article does not take the common aileron control approach. Since this sort of vehicle have a strong reverse effect, the controller command RCS system to generate sideslip angle by its yaw moment and then motivates roll moment with the desired direction by the reverse effect to tracking the bank angle command.

The lateral control strategy diagram at large angle of attack and low dynamic pressure situation is shown in Fig. (6) and Fig. (7):

##### 4.2.2. High Dynamic Pressure: Aileron Only Control Strategy

As analyzed before, the Dutch roll mode of the object vehicle is unstable at high Mach numbers which greater than 22, and its damping is very small in the whole entry process. When the flight height decreases, although LCDP varies with angle of attack, but remains negative, the aileron efficiency also increases significantly with dynamic pressure. Consequently disconnect RCS loop in this phase and deflect

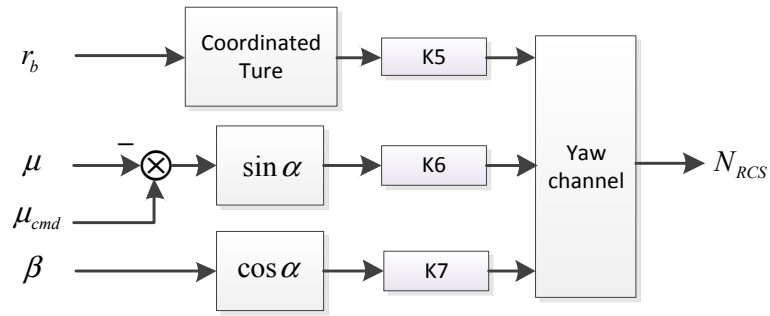


Fig. (7). The yaw channel control strategy (low dynamic pressure).

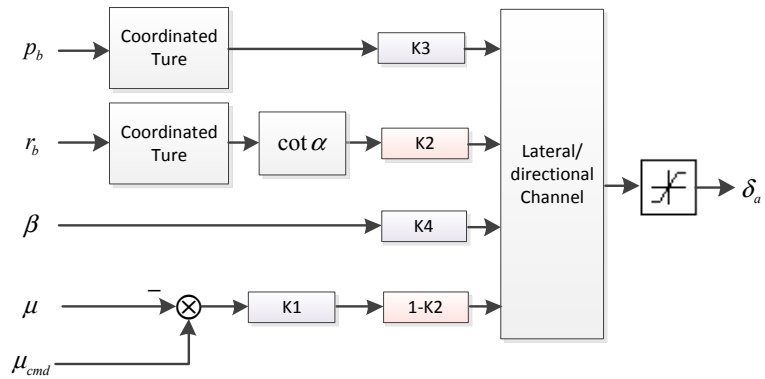


Fig. (8). The lateral/directional control strategy (high dynamic pressure).

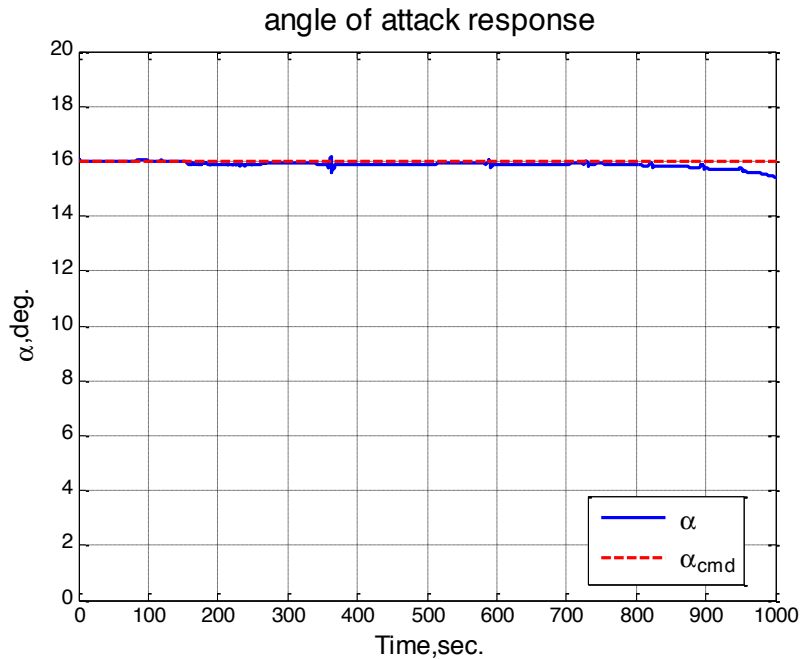


Fig. (9). The six-degree of freedom simulation result: angle of attack response.

aileron to generate sideslip angle resulting in rolling moment to control roll motion. As shown in Fig. (8), the yaw rate feedback is used to offset the motion coupling. The Dutch roll stabilization is realized through roll rate feedback.

### 5. SIMULATION RESULTS

In this section the six-degree simulation of tracking the nominal trajectory will be taken to verify the feasibility of

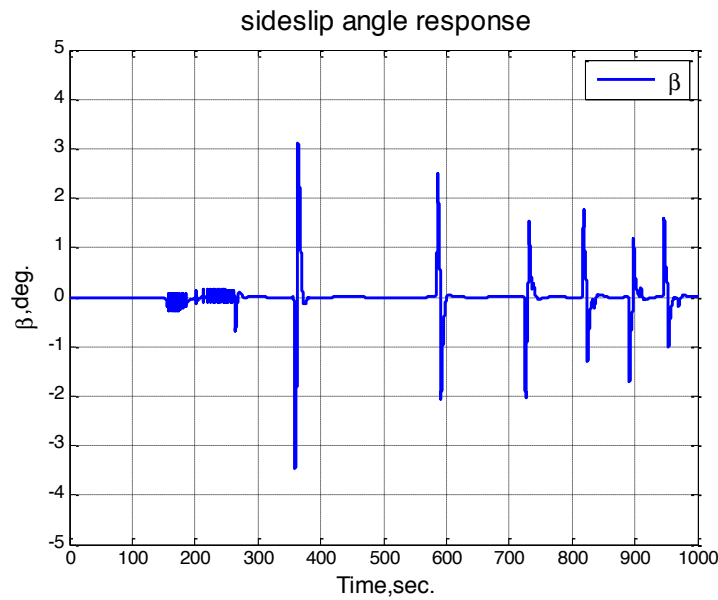


Fig. (10). The six-degree of freedom simulation result: sideslip angle response.

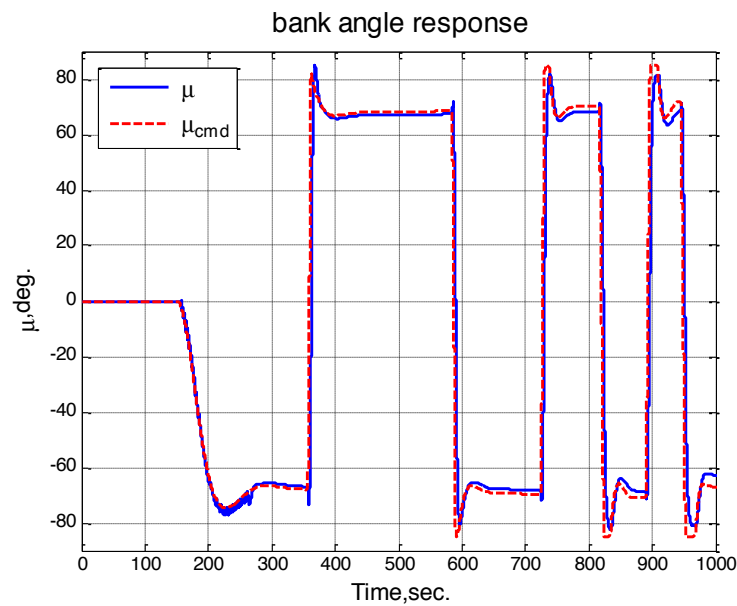


Fig. (11). The six-degree of freedom simulation result: bank angle response.

the control strategy proposed before. The attitude commands from guidance system including angle of attack command  $\alpha_{cmd}$  and bank angle command  $\mu_{cmd}$  in the simulation model. Beside follow these commands the sideslip angle need to be stabilized to around zero.

The control strategy shifting time is decided by the current dynamic pressure: in the beginning of the reentry the body flaps-RCS hybrid control strategy is adopted, with the dynamic pressure increases and actuator efficiency enhance, RCS quit from control system gradually. In the whole

reentry phase, the angle of attack command maintains at 16 degree and the bank angle command is shown in Fig. (11). The simulation step time is 0.005s and the terminal condition is  $H < 32km$ , the simulation results are shown as follows:

The Fig. (9) to Fig. (11) show that the angle of attack and bank angle command can be accurately responded and the sideslip angle maintained within  $\pm 3^\circ$ . The Fig. (12) illustrates that the aerodynamic actuators have not saturated and having a certain control margin. The Fig. (13) expresses that attitude angular rates are controlled within a reasonable range. The RCS jets total open time is 13.7 seconds.

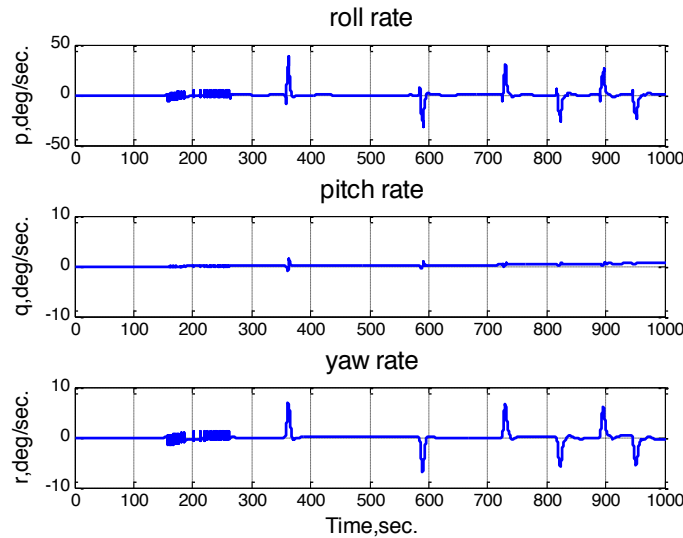


Fig. (12). The six-degree of freedom simulation result: angular rate curve.

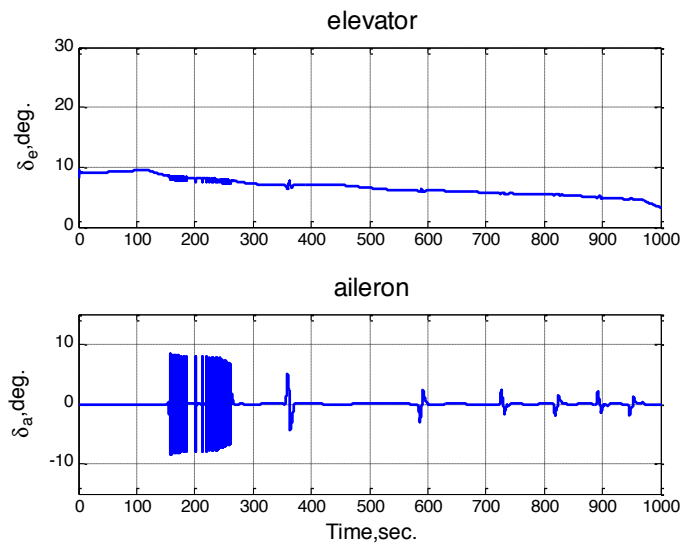


Fig. (13). The six-degree of freedom simulation result: actuators deflection curve.

## CONCLUSION

In this paper, a mathematical model is established for the analysis of RLV movement and attitude control system design, and some operating points from the trajectory are selected and linearized on them. Several common coupling mechanism in the RLV reentry process is described in detail, including the inertial coupling, the motion coupling, the Dutch roll coupling and the control coupling. Formula expression and calculation results of rapid roll stability boundary are given, and using of this rapid roll stability boundary to limit roll rate command can significantly evade inertial coupling phenomenon in the actual design of control law. A new Dutch roll's frequency prediction formula is given, and using

this method can effectively predict the Dutch roll divergent. Considering the aerodynamic characteristics of these type of aircraft, the mechanisms of motion coupling and control coupling are analyzed, and based on the above coupling characteristics the longitudinal and lateral attitude control strategy are presented, in which the body flaps and RCS are used on lateral channel when the dynamic pressure is low at high altitude, and with the height reducing and the actuator efficiency increasing only body flaps involved in attitude control. From the results of the 6 DOF simulation, it can be seen that this control strategy can accurately track the guidance command, actuator saturation haven't occur and spend less RCS propellant, which achieves the purpose of saving fuel and simplification the structure of the control system.

**CONFLICT OF INTEREST**

The authors confirm that this article content has no conflict of interest.

**ACKNOWLEDGEMENTS**

Declared none.

**REFERENCES**

- [1] T. A. Richard, *Review of X-33 Hypersonic Aerodynamic and Aerothermodynamic Development*. National Aeronautics and Space Administration Hampton va langley Research Center, 2000.
- [2] T. J. Horvath, T. F. O. Connell, F. M. Cheatwood, R. K. Prabhu, and S. J. Alter, "Experimental hypersonic aerodynamic characteristics of Mars surveyor 2001 precision lander with flap," *Journal of Spacecraft and Rockets*, vol. 43, no. 2, pp. 270-281, 2006.
- [3] A.A. Rodriguez, J.J. Dickeson, O. Cifdaloz, R. Mc Cullen, J. Benavides, S. Sridharan, A. Kelkar, J.M. Vogel, and D. Soloway, "Modeling and control of scramjet-powered hypersonic vehicles: challenges, trends, & tradeoffs," In: *AIAA Conference on Guidance, Navigation and Control*, AIAA-2008. vol. 6793, 2008.
- [4] Hall, A. Earl, "Space Transportation System." U.S. Patent No. 7,080,809, 25 Jul. 2006.
- [5] L. Huang, Z. Duan, and Y. Yang, "Several problems on control of modern aircraft," *Science & Technology Review*, vol. 26, no. 20, pp. 92-98, 2008.
- [6] E. M. Wallner, and K. H. Well. "Attitude control of a reentry vehicle with internal dynamics," *Journal of Guidance, Control, and Dynamics*, vol. 26, no. 6, pp. 846-854, 2003.
- [7] R. E. Day, *Coupling Dynamics in Aircraft: A Historical Perspective*, National Aeronautics and Space Administration, Office of Management, Scientific and Technical Information Program, vol. 532, 1997.
- [8] R. W. Kempel, *Analysis of a Coupled Roll-Spiral-Mode, Pilot-Induced Oscillation Experienced With the M2-F2 Lifting Body*. National Aeronautics and Space Administration, 1971.
- [9] G. Mengali, and G. Fabrizio, "Unified algebraic approach to approximation of lateral-directional modes and departure criteria," *Journal of Guidance, Control, and Dynamics*, vol. 27, no. 4, pp. 724-728, 2004.
- [10] F. H. Lutze, W. C. Durham, and W. H. Mason, "Unified development of lateral-directional departure criteria," *Journal of Guidance, Control, and Dynamics*, vol. 19, no. 2, pp. 489-493, 1996.
- [11] H. P. Lee, M. Chang, and M. K. Kaiser, "Flight dynamics and stability and control characteristics of the X-33 technology demonstrator vehicle," In: *AIAA Guidance, Navigation and Control Conference and Exhibit*, Boston, AIAA, 1998.
- [12] P. Calhoun, "An entry flight controls analysis for a reusable launch vehicle," In: *Proceedings of the AIAA Aerospace Sciences Meeting*, Reno, NV, 2000.

---

Received: September 16, 2014

Revised: December 23, 2014

Accepted: December 31, 2014

© Linan et al.; Licensee Bentham Open.

This is an open access article licensed under the terms of the Creative Commons Attribution Non-Commercial License (<http://creativecommons.org/licenses/by-nc/3.0/>) which permits unrestricted, non-commercial use, distribution and reproduction in any medium, provided the work is properly cited.